

# Inhibition of Alkaline Phosphatase by Cysteine: Implications for Calcium Pyrophosphate Dihydrate Crystal Deposition Disease

PAULINE P.L. SO, FLORENCE W.L. TSUI, REINHOLD VIETH, JINDRA H. TUPY, and KENNETH P.H. PRITZKER

**ABSTRACT.** *Objective.* Calcium pyrophosphate dihydrate (CPPD) crystal deposition disease, a common arthritis affecting the elderly, is characterized by the deposition of CPPD crystals in articular joints. The mechanism underlying disease expression is unknown, but factors contributing to the pathogenesis may involve changes in enzymatic activities involving pyrophosphate and phosphate metabolism. Tissue nonspecific alkaline phosphatase (TNAP) is one of the major enzymes regulating pyrophosphate concentrations in articular joints. We hypothesized that inhibition of TNAP activity at pH = 7.4 by endogenous molecules can lead to CPPD disease pathogenesis.

*Methods.* We investigated the inhibitory effects of the amino acid cysteine on TNAP's phosphatase, inorganic pyrophosphatase, and CPPD crystal dissolution activities. Kinetic parameters  $V_{\max}$ ,  $K_M$ , concentration for 50% inhibition ( $I_{50}$ ), inhibitor constant ( $K_I$ ), and specific activities calculated from Initial Velocity, Eadie-Hofstee, Simple, Dixon, and Secondary plots were used to assess enzyme inhibition.

*Results.* Cysteine inhibited TNAP's phosphatase activity uncompetitively and its inorganic pyrophosphatase activity mix-competitively. CPPD crystal dissolution activity was also inhibited.  $I_{50}$  values demonstrated that high cysteine concentration is required to inhibit 50% of enzyme activity.  $K_I$  values suggested that inorganic pyrophosphatase activity is inhibited more than the phosphatase activity.  $Ca^{++}$  and  $Mg^{++}$  ion concentrations may regulate this inhibition.

*Conclusion.* The control of endogenous inhibitors, such as cysteine, that interfere with TNAP's ability to regulate CPPD crystal formation and dissolution in joints could be a potential therapeutic option for CPPD crystal deposition disease. (First Release May 15 2007; J Rheumatol 2007;34:1313–22)

## Key Indexing Terms:

ALKALINE PHOSPHATASE  
CALCIUM PYROPHOSPHATE

CYSTEINE  
ARTHRITIS

AMINO ACIDS  
CARTILAGE

Crystals such as calcium pyrophosphate dihydrate (CPPD), monosodium urate, and calcium apatite form in biologic extracellular matrices under specific conditions. The phase, size, and habits of these crystals are highly dependent on the nature of the extracellular molecules present. Apatite crystals have been implicated in arthropathy at sites where apatite calcification has been widely recognized, such as rotator cuff bursa, but their significance in osteoarthritis (OA) or in association with CPPD crystal deposition remains controversial.

Calcium pyrophosphate dihydrate crystal deposition disease (CPPDD or pseudogout) commonly affects the elderly. CPPD crystals can be found in some patients with OA. While the relationships between CPPDD and OA are controversial, it is clear that the mechanisms of CPPD crystal deposition and the mechanisms that promote cartilage matrix changes in OA are different<sup>1</sup>. Although considerable research attention has been paid to the basic mechanisms of OA, fewer studies have been conducted in CPPDD. This is because, although CPPDD is known to occur spontaneously in other species, including non-human primates, as yet there is no animal model for this disease<sup>2,3</sup>. Currently, our understanding of the underlying disease processes in CPPDD remains limited. CPPD crystal deposition is restricted to articular connective tissues, preferentially affecting fibrocartilage, hyaline cartilage, and tissues such as synovium and intervertebral disc that undergo fibrocartilaginous metaplasia. Once formed, the CPPD crystals are very insoluble ( $K_{sp} 3 \times 10^{-18}$  mol/l)<sup>4</sup>. Although hydroxyapatite (HA) is intrinsically less soluble ( $K_{sp} 2.0 \times 10^{-59}$  mol/l)<sup>5</sup> compared to CPPD, the solubility constants are determined under controlled conditions and do not necessarily reflect that apatite solubility increases rapidly at acidity lower than pH 6.9. Further, the presence of enzymes *in vivo* alters the equi-

From the Department of Pathology and Laboratory Medicine, Mount Sinai Hospital; Department of Laboratory Medicine and Pathobiology, and Department of Immunology, University of Toronto; and Department of Cell and Molecular Biology, Toronto Western Research Institute, Toronto, Ontario, Canada.

P.P.L. So, MSc; R. Vieth, PhD, Professor; J.H. Tupy, MSc; K.P.H. Pritzker, MD, FRCPC, Professor, Department of Pathology and Laboratory Medicine, Mount Sinai Hospital, Department of Laboratory Medicine and Pathobiology, University of Toronto; F.W.L. Tsui, PhD, Associate Professor, Department of Cell and Molecular Biology, Toronto Western Research Institute.

Address reprint requests to Dr. K.P.H. Pritzker, Pathology and Laboratory Medicine, Mount Sinai Hospital, 600 University Avenue, Room 6-500-1, Toronto, Ontario M5G 1X5, Canada. E-mail: kpritzker@mtsinai.on.ca  
Accepted for publication February 9, 2007.

Personal non-commercial use only. The Journal of Rheumatology Copyright © 2007. All rights reserved.

librium conditions in physiological fluids, thereby increasing the actual solubility of CPPD<sup>6,7</sup>. Therapy for this very common disorder remains nonspecific, primarily using antiinflammatory and analgesic drugs.

Inorganic pyrophosphate (PPi) has been shown to play an important role in regulating mineralization<sup>8</sup>. PPi is strongly adsorbed to HA crystals and this adsorption prevents the further addition of calcium and phosphate ions to the crystal lattice from solution. We found that the [Pi]/[PPi] ratio is an extremely important determinant of the crystal phase formed. CPPD forms when [Pi]/[PPi] is < 3 and HA forms when [Pi]/[PPi] is > 100<sup>9</sup>. Pyrophosphate (PPi) metabolism is common to all cells. Sources of PPi for the cartilage extracellular matrix include transport of PPi from within the cell through the cell membrane in association with membrane transport systems that may involve the ANK protein<sup>8,10,11</sup>, and generation of PPi at the cell surface by tissue nonspecific alkaline phosphatases (TNAP) or ectonucleotidases, principally NPP-1<sup>12-15</sup>. The concentration of PPi in most tissues and in serum is tightly regulated. Serum [PPi] = 1–5  $\mu\text{M}$ <sup>16</sup> is far below the minimum concentration of 70–200  $\mu\text{M}$  [PPi] required for CPPD crystal formation<sup>17</sup>.

Alkaline phosphatase (ALP) is a glycoprotein and an ectoenzyme that is attached to the outer cell membrane via a phosphatidyl-inositol linkage<sup>18</sup>. The enzyme is released into soluble form by phospholipase V<sup>19,20</sup>. Structurally, ALP exists as a tetramer of 4 identical subunits (subunit MW = 64 kDa) on cell membranes but mainly as a dimer when released into extracellular fluid such as sera and synovial fluid<sup>19</sup>. The crystal structure of placental ALP revealed that mammalian ALP has 5 highly conserved regions: active site, active site valley, homodimer interface, crown region, and metal binding region<sup>21,22</sup>. The ALP active site carries the Zn<sup>++</sup> and Mg<sup>++</sup> ions that define ALP's metalloenzyme properties. The active site valley region, which extends on both sides of the active site pocket, carries hydrophobic residues that may be important in directing substrates to the active site. These residues may also play a role in stabilizing various inhibitors, resulting in the differential inhibition of ALP isoenzymes<sup>23,24</sup>. The homodimer interface is important in stabilizing and holding the subunits of ALP together as a functional dimer structure. ALP are allosteric enzymes. When the 2 subunits of ALP are not metallated, the 2 monomers cooperate negatively with each other. When they are fully metallated with Zn<sup>++</sup> coordinating to amino acids at the active sites, their catalytic activities are independent of each other, although the stability and catalytic activities of one subunit are still dependent on the conformation of the other monomer<sup>25</sup>. The crown region contains a flexible loop that may be important in ALP to collagen binding<sup>26</sup>. The metal binding region may be important in calcium to ALP binding. The most severe forms of hypophosphatasia have various mutations in the conserved regions of ALP, suggesting that TNAP plays an important role in skeletal maturation and mineralization<sup>27</sup>.

L-homoarginine, levamisole, and theophylline are 3 common small-molecule TNAP inhibitors<sup>24</sup>. However, the inhibition is uncompetitive in type. These inhibitors have low binding affinity to TNAP and are not entirely specific for TNAP. As a first step to developing improved, selective, and drug-like TNAP inhibitors, Millan's group has determined the residues that dictate the binding specificity of uncompetitive inhibitors to TNAP<sup>24</sup>. For example, residue 108 in TNAP largely determines the specificity of inhibition by L-homoarginine, and the conserved Tyr-371 is also required for L-homoarginine binding<sup>24</sup>. However, previous enzyme kinetics investigations were usually carried out using the substrate p-nitrophenyl phosphate (pNPP) at pH = 9.8<sup>28-34</sup>. It is unclear whether these results are relevant to inhibition of TNAP at physiological conditions (pH = 7.4).

We hypothesize that the inorganic pyrophosphatase activity (PPiase), i.e., degradation of PPi to Pi (PPi  $\rightarrow$  2Pi) by TNAP, is one of the key regulators of PPi concentrations, [PPi], in articular cartilage. In susceptible individuals, inhibitors of TNAP PPiase activity could raise [PPi], facilitate CPPD crystal formation, and directly inhibit CPPD crystal dissolution<sup>35</sup>. Endogenous molecules that can inhibit TNAP in articular cartilage are of particular interest. Previous reports showed that certain amino acids inhibited ALP's phosphatase activity at pH = 9.8<sup>28-34</sup>. However, the effect of these amino acids on TNAP's inorganic pyrophosphatase and CPPD crystal dissolution activity has not been well investigated, especially in physiologic conditions. Cysteine is the most interesting molecule in terms of CPPDD<sup>36-39</sup>. This amino acid has a thiol group that serves as one of the primary sources of inorganic sulfate in the body, thereby contributing to most of the glycosaminoglycan sulfate content in articular cartilage<sup>40</sup>. The amino acid also has metal coordinating and binding properties that allow it to modify proteins and alter enzyme activity<sup>41</sup>. Moreover, cysteine plays a crucial role in oxidative regulation by acting as a rate-limiting factor for glutathione synthesis<sup>41,42</sup>. To examine TNAP's potential relationship to CPPD formation and dissolution, we assessed the effects of cysteine on TNAP's phosphatase, inorganic pyrophosphatase, and CPPD crystal dissolution activity at near-physiologic conditions: pH = 7.4, [Ca<sup>++</sup>] = [Mg<sup>++</sup>] = 1 mM.

## MATERIALS AND METHODS

**Phosphatase (Piase) assay.** Cysteine (Sigma Chemical Co.) at 0, 1, 10, and 100 times physiological concentration (0, 40, 400, 4000  $\mu\text{M}$ ) was mixed with substrate pNPP (Sigma) at 0, 5, 25, 50, 100, 250, 500, 1000, and 2000  $\mu\text{M}$  in wells of 96-well microtiter plates (Corning CoStar). In adult humans, the average plasma concentration of cysteine is about 40  $\mu\text{mol/l}$ . This value was calculated by taking the average of the highest and lowest number in the reference range of men and women<sup>43</sup>. [Ca<sup>++</sup>] = 1 mM and [Mg<sup>++</sup>] = 1 mM, two of the major ions in humans, were also added to the systems to mimic physiologic conditions. All solutions were made with Tris-HCl, pH 7.4 (Sigma). Kidney ALP (200 U/l; Calzyme) was added to each well and the plates were incubated at 37°C for 10 min. The reaction was stopped by addition of 0.01 M NaOH (Fisher Scientific). The plates were read at 405 nm on a plate reader (Bio-Tek Instruments, model E1311). The results were expressed as the

nmol of p-nitrophenol generated/unit ALP/min. At least 4 sets of experiments were performed and each set was done in duplicate.

**Pyrophosphatase (PPiase) assay.** Cysteine at 0, 1, 10 and 100 times physiological concentration (0, 40, 400, 4000  $\mu$ M) was mixed with substrate PPi at concentrations corresponding to pNPP for phosphatase assay. The method for the PPiase assay was similar to that of the Piase assay. The protocol differed by the addition of a color reagent of 5%  $\text{FeSO}_4$  (Caledon) and 1% ammonium molybdate (BDH Ltd.) in 1 N  $\text{H}_2\text{SO}_4$  (Van Waters and Rogers Inc.) instead of 0.01 M NaOH at the end of the 10 min incubation, and by reading microtiter plates at 630 nm instead of 405 nm.

**Preparation of CPPD crystals.** CPPD (M) crystals were prepared using described methods<sup>44</sup>. The CPPD (M) crystal phase was confirmed by powder x-ray diffraction analysis using a Rigaku Multiflex X-Ray Diffractometer. Under polarized light microscopy, the CPPD (M) crystals synthesized had needle shapes and ranged from 1 to 20  $\mu$ m in length<sup>44</sup>.

**CPPD crystal dissolution assay.** Cysteine at 0, 1, 10, and 100 times physiological concentration (0, 40, 400 and 4000  $\mu$ M) was mixed with kidney ALP (200 U/l) and CPPD crystals (100  $\mu$ g) in 2 ml microcentrifuge tubes.  $\text{Ca}^{++}$  and  $\text{Mg}^{++}$  ion concentrations ( $[\text{Ca}^{++}]$ ,  $[\text{Mg}^{++}]$ ) were also added to the systems accordingly. All solutions were made with Tris-HCl, pH 7.4. The mixtures were incubated at 37°C for 2 h with gentle rocking using a test tube rocker (Johns Scientific Thermolyne Speci-Mix, 20 rpm) to prevent sedimentation of crystals at the bottom of the tubes. After incubation, crystals were spun down at 1400 rpm in a microcentrifuge (Eppendorf Centrifuge Model 5412). Thereafter, the methods for measuring the amount of phosphate released were the same as those outlined in the PPiase assay.

**Data analysis.**  $V_{\max}$  and  $K_M$  were calculated from Initial Velocity plots (Velocity vs [substrate]) by the computer curve-fitting program Kaleidagraph (Synergy, MS Windows Version 3.6X)<sup>45,46</sup>, which uses a nonlinear least-square method from the Levenberg-Marquardt algorithm to fit equations of curves to data points<sup>47</sup>. Eadie-Hofstee plots (Velocity vs Velocity/[substrate]) give  $V_{\max}$  and  $K_M$  values, and in this study we chose these plots to display enzyme kinetics based on the shape of the graphs, as they most clearly illustrate the different types of enzymatic inhibition<sup>48</sup>.  $I_{50}$  values, which represent the concentration of inhibitor needed to inhibit 50% of ALP activity, were derived from the x-intercepts of the plotted lines from Simple ([Substrate]/Velocity vs [inhibitor])<sup>49,50</sup> and Dixon (1/Velocity vs [inhibitor]) plots<sup>51</sup>. The  $K_i$  values, which represent the inhibitor constant or the association of enzyme to an inhibitor, were derived from the y-intercept of Secondary plots (1/ $I_{50}$  vs  $V_o/V_{\max}$ )<sup>49,50</sup>.

**Statistical analysis.** Statistical analyses were conducted using the computer program SPSS (v. 12.0.1). Differences in the enzyme kinetic parameters were tested using analysis of variance (ANOVA) followed by post-hoc Dunnett T test. The Dunnett T test compares values between a control group (no amino acid present) and its test groups (groups when amino acids are present). Using a 2-tail test, a p value < 0.05 is regarded as statistically significant.

## RESULTS

The inhibitory activity of cysteine on TNAP's Piase and PPiase activity was assessed using Initial Velocity and Eadie-Hofstee plots. Typically, Initial Velocity plots were used to calculate  $V_{\max}$  (maximum reaction velocity at substrate concentration when enzyme is saturated), and  $K_M$  (substrate concentration at 1/2  $V_{\max}$ ). The type of enzyme inhibition was determined by the Eadie-Hofstee plots.

Representative Initial Velocity and Eadie-Hofstee plots of TNAP's Piase activity with cysteine are shown in Figure 1. The plots indicate that the amino acid is an uncompetitive inhibitor under the various  $[\text{Ca}^{++}]$  and  $[\text{Mg}^{++}]$  conditions.  $V_{\max}$  and  $K_M$  values generated from the Initial Velocity plots by the Kaleidagraph program in Table 1 are consistent with

these findings, namely both  $V_{\max}$  and  $K_M$  values decrease with increasing cysteine concentration. Some of the results are significant at physiologic concentrations of cysteine and all results are significant at 10 $\times$  the physiologic concentration of cysteine. Note that at 100 $\times$  physiologic concentration of cysteine,  $K_M$  values start to increase again, except when both  $[\text{Ca}^{++}]$  and  $[\text{Mg}^{++}]$  are present. This suggests that the mechanism of cysteine inhibition may be regulated by its concentration and the presence of ionic metals in the vicinity.

Initial Velocity and Eadie-Hofstee plots of TNAP's PPiase activity with cysteine are shown in Figure 2. The plots indicate that the amino acid is a competitive or mixed-competitive inhibitor under the various  $[\text{Ca}^{++}]$  and  $[\text{Mg}^{++}]$  conditions.  $V_{\max}$  and  $K_M$  values generated by Kaleidagraph in Table 2 are consistent with these findings, namely  $K_M$  increases with increasing cysteine concentration, while  $V_{\max}$  decreases (mixed-competitive inhibition), or in the case with no  $\text{Ca}^{++}$  and  $\text{Mg}^{++}$  ions present, it stays constant (competitive inhibition). However, these changes are significant only at high cysteine concentrations. Nevertheless, the result of particular interest in this assay is the abrupt drop in  $V_{\max}$  and  $K_M$  values in the presence of both  $[\text{Ca}^{++}]$  and  $[\text{Mg}^{++}]$ . This drop in kinetic parameters may indicate that regulation of TNAP activity between 400  $\mu$ M and 4000  $\mu$ M cysteine may have been breached. Further investigation is required to identify the regulating factor between these 2 cysteine concentrations in the presence of  $[\text{Ca}^{++}] = [\text{Mg}^{++}] = 1$  mM.

Inhibition by cysteine of TNAP's Piase and PPiase activity was also assessed using Simple, Dixon, and Secondary plots. Simple plots give a set of lines where each line represents a specific substrate concentration. The point at which each line crosses the x-axis is the  $I_{50}$  value, or the concentration of cysteine needed to inhibit 50% of TNAP activity at that substrate concentration. The arrangement of lines around the x-axis can also help identify the type of enzyme inhibition. Dixon plots also make use of an arrangement of lines to determine  $I_{50}$  values and the type of inhibition. Often, Dixon plots are used to complement Simple plots when they are unclear<sup>49-51</sup>.

$I_{50}$  values for the Piase and PPiase assays (data not shown) are interpolated from Simple plots. It appears that very high concentrations are required to inhibit 50% of TNAP activity. For some of the assays, the amount of cysteine required for inhibition increases as the concentration of substrate increases. This is typical for competitive and mixed inhibitions, where the inhibitor has to compete with the substrate for the active site of the enzyme. The question whether cysteine can accumulate to such high concentrations in articular cartilage remains unanswered. However, it may not be necessary for cysteine to inhibit TNAP to 50% of its activity to cause CPPD crystal deposition. On the other hand, in the PPiase assay with  $[\text{Ca}^{++}] = [\text{Mg}^{++}] = 1$  mM present, it appears that less cysteine is required to inhibit 50% of TNAP activity as substrate concentration increases. This finding usually occurs in uncompetitive competition. In this system, there was an abrupt drop in

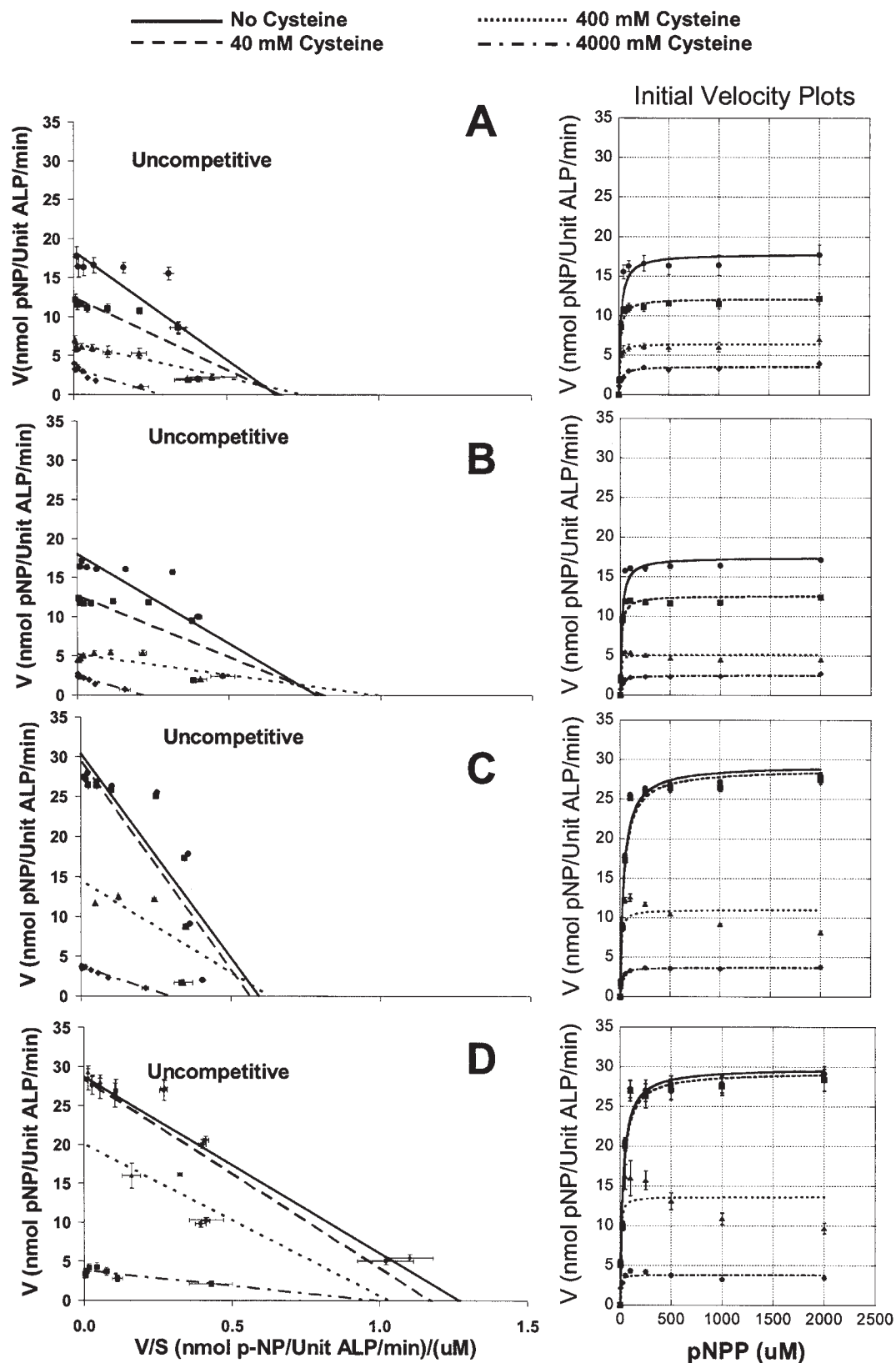


Figure 1. Representative Eadie-Hofstee and Initial Velocity plots of TNAP phosphatase activity under various buffer conditions. In all conditions, (A) cysteine only, (B) cysteine with  $[Ca^{++}] = 1$  mM, (C) cysteine with  $[Mg^{++}] = 1$  mM, and (D) cysteine with  $[Ca^{++}] = [Mg^{++}] = 1$  mM, plots show uncompetitive inhibition of TNAP phosphatase activity where both  $V_{max}$  and  $K_M$  decrease.  $V_{max}$  and  $K_M$  were determined by the Kaleidagraph curve-fitting program.



Table 1. Kinetic parameters  $V_{\max}$  and  $K_M$  of TNAP phosphatase assay under various  $[Ca^{++}]$  and  $[Mg^{++}]$  conditions. At least 4 sets of experiments were performed in duplicates. Values are expressed in mean  $\pm$  SD.

| [Cysteine], $\mu$ M | $[Ca^{++}] = [Mg^{++}] = 0$ mM |             | $[Ca^{++}] = 1$ mM |                | $[Mg^{++}] = 1$ mM |                | $[Ca^{++}] = [Mg^{++}] = 1$ mM |                |
|---------------------|--------------------------------|-------------|--------------------|----------------|--------------------|----------------|--------------------------------|----------------|
|                     | $V_{\max}$                     | $K_M$       | $V_{\max}$         | $K_M$          | $V_{\max}$         | $K_M$          | $V_{\max}$                     | $K_M$          |
| 0                   | 18 $\pm$ 2                     | 19 $\pm$ 1  | 17.4 $\pm$ 0.4     | 15.6 $\pm$ 0.3 | 29.3 $\pm$ 0.7     | 35 $\pm$ 2     | 30 $\pm$ 2                     | 27 $\pm$ 1     |
| 40                  | 12 $\pm$ 1*                    | 13 $\pm$ 1* | 12.6 $\pm$ 0.5*    | 11 $\pm$ 1*    | 29 $\pm$ 1         | 36 $\pm$ 4     | 29 $\pm$ 3                     | 28 $\pm$ 2     |
| 400                 | 6 $\pm$ 1*                     | 9 $\pm$ 4*  | 5.1 $\pm$ 0.2*     | 4.2 $\pm$ 0.6* | 11 $\pm$ 0.3*      | 8.3 $\pm$ 0.6* | 14 $\pm$ 2*                    | 4.8 $\pm$ 0.9* |
| 4000                | 3.6 $\pm$ 0.3*                 | 24 $\pm$ 5  | 2.5 $\pm$ 0.4*     | 15 $\pm$ 4     | 3.7 $\pm$ 0.2*     | 14 $\pm$ 2*    | 3.8 $\pm$ 0.9*                 | 5 $\pm$ 2*     |

\* Calculated value with cysteine present in the system is statistically significant at the  $p < 0.05$  level from calculated value with no cysteine in the system.

$K_M$  value as the concentration of cysteine increased. These findings suggest that cysteine inhibits TNAP PPIase activity readily as pyrophosphates accumulate in the extracellular matrix.

Secondary plots can also be used to determine types of enzyme inhibition. In addition, the y-intercepts ( $1/K_{IC}$ ) and slopes ( $1/K_{IU} - 1/K_{IC}$ ) of Secondary plots represent  $K_I$  values (inhibitor constant) that are used to determine the degree of enzyme inhibition<sup>49,50</sup>.  $K_I$  measures the association of inhibitors to enzymes. Inhibitors with small  $K_I$  values are strong inhibitors, while those with large  $K_I$  values are weak inhibitors.

Inhibitor constant ( $K_I$ ) values for both TNAP's Piase and PPIase assays interpolated from Secondary plots are shown in Table 3. Between the 2 assays, it appears that cysteine inhibits TNAP PPIase activity better than its Piase activity. Most interestingly, cysteine inhibits TNAP PPIase activity best (lowest  $K_I$  value) when  $[Ca^{++}] = 1$  mM and  $[Mg^{++}] = 1$  mM are both present in the system, while it inhibits TNAP Piase activity the least (largest  $K_I$  value) under the same conditions. This implies that  $[Ca^{++}]$  and  $[Mg^{++}]$  may help regulate the inhibition of TNAP activity by cysteine and that TNAP pyrophosphatase activity may be more important at physiologic pH.

Table 4 shows the specific activities for the CPPD crystal dissolution assays of cysteine under various conditions of  $[Ca^{++}]$  and  $[Mg^{++}]$ . In all cases, the specific activity of TNAP was significantly inhibited when cysteine concentration was at 100 $\times$  its physiological concentration. In the presence of  $[Ca^{++}]$  only, the activity of TNAP was inhibited even in the absence of cysteine, suggesting that  $[Ca^{++}] = 1$  mM is a strong inhibitor of TNAP. In a system of both PPI and  $Ca^{++}$  dysregulation, the formation of CPPD crystals will be highly favorable.

## DISCUSSION

Many different types of TNAP inhibitors have been reported in the literature, but amino acids are of the most interest since they are present endogenously in the body. Bodansky first reported inhibition of ALP by glycine<sup>28</sup>, lysine<sup>29</sup>, and histidine<sup>29</sup> in the 1940s. Fishman, *et al* followed on this work and found that homoarginine<sup>30-32</sup>, phenylalanine<sup>32,33</sup>, and tryptophan<sup>32,34</sup> differentially inhibit different ALP isozymes.

Inhibition of TNAP's phosphatase and inorganic pyrophosphatase activities by cysteine was first reported in the 1960s by Cox and Macleod when it was found that culture medium with cysteine slowed the activities of the enzyme in human cell cultures<sup>36</sup>. Later reports showed that cysteine and some of its analogs also inhibit the enzyme<sup>37-39</sup>. In contrast, we observed that related molecules such as serine, cysteamine, and glutathione have no inhibitory effect on TNAP (data not shown). Most studies have been focused on the inhibition of TNAP's phosphatase activity at alkaline pH. Very few studies have measured the inhibition of TNAP activity at the physiological pH of 7.4, and fewer studies examined the inhibition of TNAP's inorganic pyrophosphatase activities. To our knowledge, this is the first study reporting the effects of amino acids on TNAP's CPPD crystal dissolution activities. This is not surprising; 40 years ago when TNAP was first identified to have a primary phosphoester hydrolysis function at alkaline pH<sup>52,53</sup>, the association of TNAP with CPPD crystal dissolution was unknown. It was not until recently when TNAP inorganic pyrophosphatase was reexamined that the enzyme was found to possess CPPD crystal dissolution capability as well<sup>6,7,54</sup>. Indeed, TNAP as well as inorganic pyrophosphatase needs to be in close proximity to the crystal surface for dissolution to proceed<sup>54,55</sup>.

Our results showed that cysteine does inhibit the various catalytic activities of TNAP under near-physiologic conditions. However, most of the inhibition of TNAP activity was significant only at high cysteine concentrations (at 100 $\times$  physiologic plasma concentration of cysteine, or 4000  $\mu$ M cysteine). Although it may seem unlikely that cysteine can accumulate at such high amounts in the bloodstream, the unique architecture and highly viscous environment of the articular cartilage may prove to be a special circumstance for cysteine concentration. Moreover, the cysteine concentration used for our study was an average value taken from the reference range for adult humans; thus, it is likely there are people with higher than the average cysteine concentration. Similarly, the daily biological variations in amino acid content could vary considerably, especially after a meal with high protein content. In addition, elevated amino acids have been found in the synovial fluid of patients with various arthritic conditions, including CPPD. However, the only amino acids tested to date have

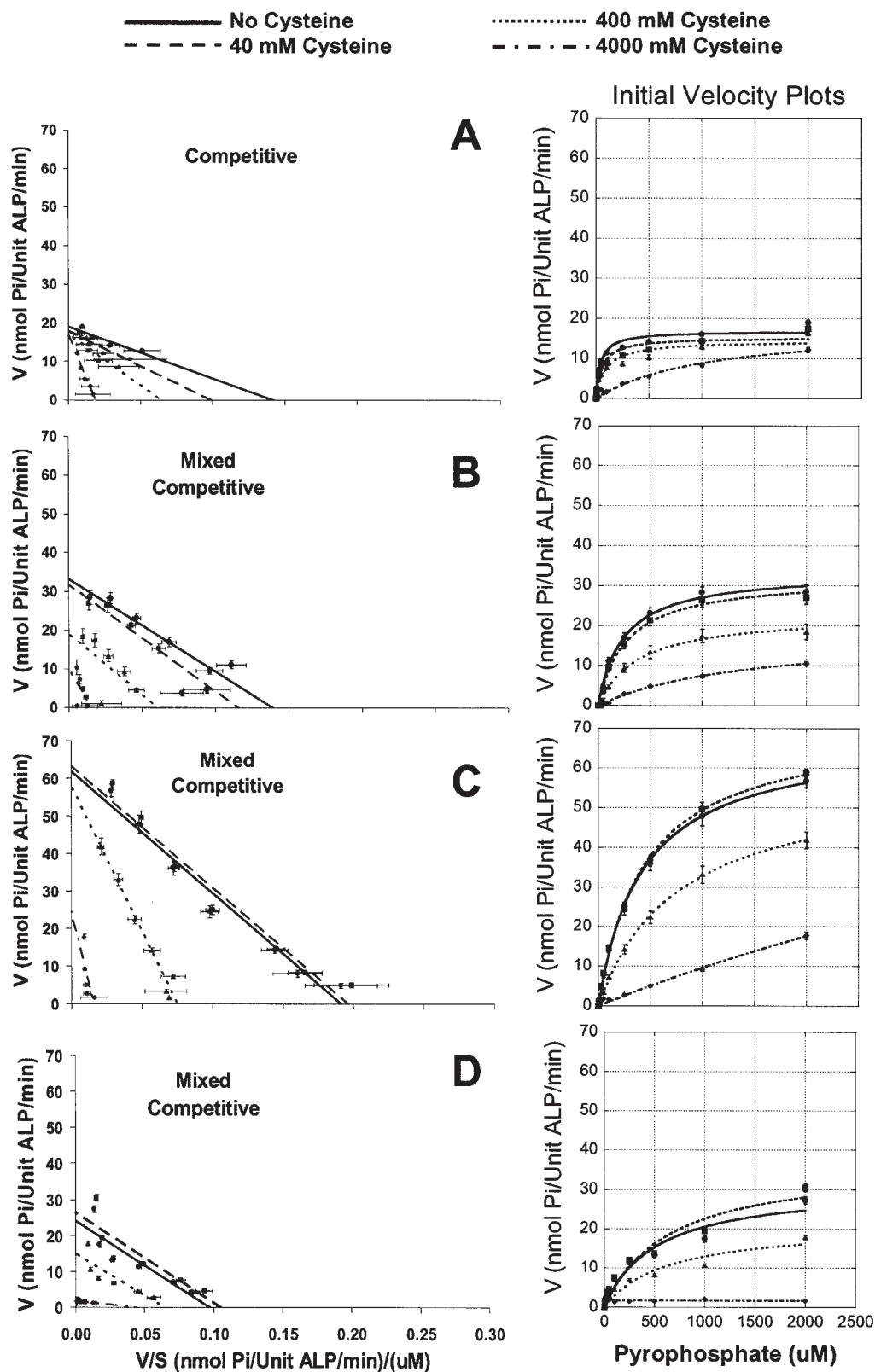


Figure 2. Representative Eadie-Hofstee and Initial Velocity plots of TNAP pyrophosphatase activity under various buffer conditions. In all conditions, (A) cysteine only, (B) Cysteine with  $[Ca^{++}] = 1$  mM, (C) cysteine with  $[Mg^{++}] = 1$  mM, and (D) cysteine with  $[Ca^{++}] = [Mg^{++}] = 1$  mM, plots show competitive inhibition ( $V_{max}$  stays constant while  $K_M$  increases) and mixed-competitive inhibition ( $V_{max}$  decreases while  $K_M$  increases) of TNAP pyrophosphatase activity.

Table 2. Kinetic parameters  $V_{\max}$  and  $K_M$  of TNAP phosphatase assay under various  $[Ca^{++}]$  and  $[Mg^{++}]$  conditions. At least 4 sets of experiments were performed in duplicates. Values are expressed in mean  $\pm$  SD.

| [Cysteine], $\mu$ M | $[Ca^{++}] = [Mg^{++}] = 0$ mM |                | $[Ca^{++}] = 1$ mM |                 | $[Mg^{++}] = 1$ mM |                  | $[Ca^{++}] = [Mg^{++}] = 1$ mM |               |
|---------------------|--------------------------------|----------------|--------------------|-----------------|--------------------|------------------|--------------------------------|---------------|
|                     | $V_{\max}$                     | $K_M$          | $V_{\max}$         | $K_M$           | $V_{\max}$         | $K_M$            | $V_{\max}$                     | $K_M$         |
| 0                   | 16.8 $\pm$ 0.6                 | 39 $\pm$ 13    | 34 $\pm$ 4         | 243 $\pm$ 29    | 69 $\pm$ 2         | 439 $\pm$ 102    | 32 $\pm$ 3                     | 529 $\pm$ 112 |
| 40                  | 15.3 $\pm$ 0.4                 | 58 $\pm$ 11    | 32 $\pm$ 3         | 276 $\pm$ 232   | 72 $\pm$ 2         | 453 $\pm$ 81     | 38 $\pm$ 5                     | 685 $\pm$ 230 |
| 400                 | 15 $\pm$ 1                     | 87 $\pm$ 57    | 23 $\pm$ 4         | 402 $\pm$ 60    | 58 $\pm$ 6         | 731 $\pm$ 280    | 22 $\pm$ 4*                    | 694 $\pm$ 315 |
| 4000                | 19 $\pm$ 3                     | 949 $\pm$ 604* | 19 $\pm$ 8*        | 1493 $\pm$ 637* | 29 $\pm$ 13*       | 2103 $\pm$ 1441* | 2.0 $\pm$ 0.4*                 | 1 $\pm$ 1*    |

\* Calculated value with cysteine present in the system is statistically significant at the  $p < 0.05$  level from calculated value with no cysteine in the system.

Table 3. Inhibitor constants ( $K_I$ ) measuring affinity of cysteine to TNAP from TNAP phosphatase and pyrophosphatase assays under various  $[Ca^{++}]$  and  $[Mg^{++}]$  conditions. At least 4 sets of experiments were performed in duplicates. Values are expressed in mean  $\pm$  SD. Low  $K_I$  values indicate high affinity of enzyme to inhibitor. High  $K_I$  values indicate low affinity of enzyme to inhibitor.

| Assay Condition                                | Inhibitor Constant ( $K_I$ ) Values |                       |
|--|-------------------------------------|-----------------------|
|  | Phosphatase Assay                   | Pyrophosphatase Assay |
| Cysteine only (no $[Ca^{++}]$ or $[Mg^{++}]$ ) | 1900 $\pm$ 110                      | 770 $\pm$ 190         |
| Cysteine with $[Ca^{++}] = 1$ mM               | 380 $\pm$ 180                       | 650 $\pm$ 47          |
| Cysteine with $[Mg^{++}] = 1$ mM               | 2600 $\pm$ 490                      | 580 $\pm$ 300         |
| Cysteine with $[Ca^{++}] = [Mg^{++}] = 1$ mM   | 3000 $\pm$ 1600                     | 270 $\pm$ 99          |

Table 4. Specific activities from TNAP CPPD crystal dissolution experiments under  $[Ca^{++}]$  and  $[Mg^{++}]$  buffer conditions. Specific activities are expressed in units of nmol of phosphate generated/unit ALP/min. Four sets of experiments were performed in duplicates. Values are expressed in mean  $\pm$  SD.

| [Cysteine], $\mu$ M | $[Ca^{++}] = [Mg^{++}] = 0$ mM | $[Ca^{++}] = 1$ mM | $[Mg^{++}] = 1$ mM | $[Ca^{++}] = [Mg^{++}] = 1$ mM |
|---------------------|--------------------------------|--------------------|--------------------|--------------------------------|
| 0                   | 1.1 $\pm$ 0.3                  | 0.08 $\pm$ 0.07    | 6.9 $\pm$ 0.1      | 0.46 $\pm$ 0.04                |
| 40                  | 1.1 $\pm$ 0.4                  | 0.04 $\pm$ 0.03    | 6.8 $\pm$ 0.3      | 0.49 $\pm$ 0.11                |
| 400                 | 0.79 $\pm$ 0.34                | 0.03 $\pm$ 0.04    | 6.7 $\pm$ 0.2      | 0.43 $\pm$ 0.05                |
| 4000                | 0.17 $\pm$ 0.09*               | 0.01 $\pm$ 0.08    | 5.2 $\pm$ 0.3*     | 0.15 $\pm$ 0.03*               |

\* Calculated value with cysteine present in the system is statistically significant at the  $p < 0.05$  level from calculated value with no cysteine in the system.

been excitatory amino acids that might be released into the joints during inflammation<sup>56</sup>. One study investigated the thiol pattern in plasma of subjects with rheumatoid arthritis; it was found that these patients have higher plasma concentrations of cysteine, homocysteine, protein-bound cysteine, and protein-bound homocysteine compared to controls<sup>57</sup>.

Although the exact mechanism of inhibition remains unclear, there are reports of how cysteine<sup>36-39</sup> and other amino acids<sup>22-25,55,58</sup> inhibit TNAP. Recently, a model of TNAP's structure has been created; it was found that the enzyme has 5 highly conserved regions: active site, active site valley, homodimer interface, crown region, and metal binding region<sup>22</sup>. The active site carries the  $Zn^{++}$  and  $Mg^{++}$  ions that portray ALP's metalloenzyme properties. Since cysteine has metal binding and coordinating properties, it may interact with these metals and play a role in activating and deactivating enzyme catalysis. As shown in our study, changing  $[Ca^{++}]$  and  $[Mg^{++}]$  alters the ability of cysteine to inhibit TNAP. At low  $[Ca^{++}]$  and  $[Mg^{++}]$ , the amino acid may be drawn to the metals at the active site, thereby interfering with proper enzymatic activity.

In contrast, in the presence of  $[Ca^{++}] = [Mg^{++}] = 1$  mM, cysteine may interact with free metal ions and the inhibition of enzyme is decreased. Similarly, at high concentration of cysteine and in the presence of  $[Ca^{++}] = [Mg^{++}] = 1$  mM, cysteine may sequester the  $Mg^{++}$  and  $Zn^{++}$  ions, while the  $Ca^{++}$  ions will occupy the free spaces in the active site, leading to a drastic decrease in enzymatic activity. The interaction of metals, TNAP, and cysteine is complex. At the active-site valley region of TNAP, existing hydrophobic residues may help direct substrates to the active site. These residues may also help stabilize various inhibitors, including cysteine. It is suggested that the residues may be responsible for the differential inhibition of the different isoenzymes<sup>23,24</sup>. The homodimer interface of ALP is important in stabilizing and holding the subunits of ALP together into its functional dimer structure.

There are 5 conserved cysteine residues per subunit of TNAP. Disruption of the disulfide bond between some of these residues can change the structure and prevent the formation of an active enzyme<sup>58</sup>. Thus, it is possible that with

free cysteine molecules accumulating in the environment, interaction or formation of novel disulfide bonds between the unbound cysteine and the cysteine residues in TNAP, or the reduction of disulfide bonds to thiols by cysteine, could result in decreased enzyme activity. Finally, TNAP's crown region contains a flexible loop that may be important in collagen binding, while its metal binding region is important in calcium binding. Both these regions further contribute to the role of TNAP in articular cartilage and may have a direct relationship with tissue calcification and soft tissue ossification.

Cysteine possesses an interesting metabolic pathway. It is the rate-determining step in the formation of glutathione<sup>42</sup>. If there were a block in the conversion of cysteine to glutathione, cysteine would accumulate proportionally. These conditions provide an excess of cysteine available to inhibit TNAP at the articular cartilage, favoring CPPD crystal formation. There would also be less glutathione for antioxidative protection, favoring oxidative damage at the articular joint. It is known that in the elderly (the group that comprises most patients with CPPD), serum glutathione level decreases significantly with a parallel increase in cysteine<sup>42,59,60</sup>. Degeneration of articular cartilage is a common finding in CPPD arthropathy.

Changes in glycosaminoglycan content, such as an increase in keratan sulfate and a decrease in chondroitin sulfate, have been observed in the articular cartilage of the elderly<sup>61</sup>. The same condition applies to patients with CPPD when compared to healthy individuals of the same age. Moreover, there is more chondroitin 6-sulfate than chondroitin 4-sulfate in the diseased cartilage<sup>62</sup>. Accordingly, it is thought that the architecture of the articular cartilage matrix may play a role in the pathogenesis of CPPD by promoting or inhibiting crystal growth. The focus is the free sulfate groups that are present in the keratan and chondroitin sulfates, similar to the free sulfhydryl group in cysteine's side chain. This may explain why this amino acid has the most potent effect on TNAP activity. Amino acids such as arginine, dimethyl arginine, lysine, methyl lysine, histidine, serine, and methionine have also been tested for their effects on TNAP Piase, PPIase, and CPPD crystal dissolution activity. None of these amino acids has the same degree of inhibition on TNAP as cysteine (data not shown).

Recently, ALP has been determined to be part of a superfamily that includes sulfatases<sup>63,64</sup>. *E. coli* ALP has also been shown to possess weak sulfatase activity that is more significant than the spontaneous hydrolysis of sulfates without enzymes<sup>65</sup>. There is an important interrelationship between TNAP and thiol compounds that is of particular interest for future investigations.

There are currently no specific therapies for the treatment of CPPDD. Elucidating mechanisms in which altered enzymatic activity might contribute to the pathogenesis of the disease is the key to development of novel therapeutic strategies. Our studies indicate that removal of inhibitors such as accu-

mulation of the endogenous amino acid cysteine in articular cartilage could restore previously inhibited activity of TNAP. At physiologic conditions TNAP has inorganic pyrophosphatase activity and CPPD crystal dissolution activity. Thus, restoration of ALP activity will lead to decreased CPPD crystal formation and increased CPPD crystal clearance. Consequently, upregulation of TNAP activity by removal of inhibitors or with measures to increase TNAP activity locally in cartilage may be an important target for therapeutic developments in CPPDD.

## ACKNOWLEDGMENT

The authors thank Dr. Jaro Sodek and Dr. Howard Tenenbaum for their valuable advice throughout this study and in the preparation of this article. We thank Jovil Kanampuzha for helpful input on effects of other sulfur-containing amino acid derivatives on CPPD crystal dissolution. The authors also thank Kerri Tupy for performing X-ray diffraction on CPPD crystals.

## REFERENCES

1. Pritzker KPH. Pathology of osteoarthritis. In: Brandt KD, Lohmander S, Doherty M, editors. Osteoarthritis. Oxford: Oxford University Press; 1998:106-30.
2. Chateauvert JMD, Grynblas MD, Kessler MJ, Pritzker KPH. Spontaneous osteoarthritis in rhesus macaques. II. Characterization of disease and morphometric studies. *J Rheumatol* 1990;17:73-83.
3. Kandel RA, Renlund RC, Cheng PT, Rapley WA, Mehren KG, Pritzker KPH. Calcium pyrophosphate dihydrate crystal deposition disease with concurrent vertebral hyperostosis in a Barbary ape. *Arthritis Rheum* 1983;26:682-7.
4. McCarty DJ, Palmer DW, James C. Clearance of calcium pyrophosphate dihydrate crystals in vivo. *Arthritis Rheum* 1979;22:1122-31.
5. Markovic M, Fowler BO, Tung MS. Preparation and comprehensive characterization of a calcium hydroxyapatite reference material. *J Res Natl Inst Stand Technol* 2004;109:553-68.
6. Xu Y, Cruz TF, Pritzker KPH. Alkaline phosphatase dissolves calcium pyrophosphate dihydrate crystals. *J Rheumatol* 1991;18:1606-10.
7. Xu Y, Pritzker KPH, Cruz TF. Characterization of chondrocyte alkaline phosphatase as a mediator in the dissolution of calcium pyrophosphate dihydrate crystals. *J Rheumatol* 1994;21:912-9.
8. Terkeltaub RA. Inorganic pyrophosphate generation and disposition in pathophysiology. *Am J Physiol Cell Physiol* 2001;281:C1-C11.
9. Cheng P-T, Pritzker KPH. Pyrophosphate, phosphate ion interaction: Effects on calcium pyrophosphate and calcium hydroxyapatite crystal formation in aqueous solutions. *J Rheumatol* 1983;10:769-77.
10. Goding JW, Grobbs B, Slegers H. Physiological and pathophysiological functions of the ectonucleotide pyrophosphatase/phosphodiesterase family. *Biochim Biophys Acta* 2003;1638:1-19.
11. Ryan LM, Rosenthal AK. Metabolism of extracellular pyrophosphate. *Curr Opin Rheumatol* 2003;15:311-4.
12. Graff RD, Picher M, Lee GM. Extracellular nucleotides, cartilage stress, and calcium crystal formation. *Curr Opin Rheumatol* 2003;15:315-20.
13. Picher M, Graff RD, Lee GM. Extracellular nucleotide metabolism and signaling in the pathophysiology of articular cartilage. *Arthritis Rheum* 2003;48:2722-36.
14. Tenenbaum J, Muniz O, Schumacher HR, Good AE, Howell DS. Comparison of phosphohydrolase activities from articular cartilage in calcium pyrophosphate deposition disease and primary osteoarthritis. *Arthritis Rheum* 1981;24:492-500.



15. Anderson HC, Sipe JB, Hesse L, et al. Impaired calcification around matrix vesicles of growth plate and bone in alkaline phosphatase-deficient mice. *Am J Pathol* 2004;164:841-7.
16. Silcox DC, McCarty DJ. Measurement of inorganic pyrophosphate in biological fluids. Elevated levels in some patients with osteoarthritis, pseudogout, agromegaly and uremia. *J Clin Invest* 1973;53:1863-70.
17. Pritzker KPH. Calcium pyrophosphate crystal formation and dissolution. In: Amjad Z, editor. *Calcium phosphates in biological and industrial systems*. Boston: Kluwer Academic Publishers; 1998:277-301.
18. Ogata S, Hayashi Y, Takami N, Ikehara Y. Chemical characterization of the membrane-anchoring domain of human placental alkaline phosphatase. *J Biol Chem* 1988;263:10489-94.
19. Hamilton BA, McPhee JL, Hawrylak K, Stinson RA. Alkaline phosphatase releasing activity in human tissues. *Clin Chim Acta* 1989;186:249-54.
20. Pizauro JM, Ciancaglini P, Leone FA. Characterization of the phosphatidylinositol-specific phospholipase C-released form of rat osseous plate alkaline phosphatase and its possible significance on endochondral ossification. *Mol Cell Biochem* 1995;152:121-9.
21. Millan JL. Review. Alkaline phosphatases. Structure, substrate specificity and functional relatedness to other members of a large superfamily of enzymes. *Purinergic Signalling* 2006;2:335-41.
22. Mornet E, Stura E, Lia-Baldini AS, Stigbrand T, Menez A, Le Du MH. Structural evidence for a functional role of human tissue nonspecific alkaline phosphatase in bone mineralization. *J Biol Chem* 2001;276:31171-8.
23. Hoylaerts MF, Manes T, Millan JL. Molecular mechanism of uncompetitive inhibition of human placental and germ-cell alkaline phosphatase. *Biochem J* 1992;286:23-30.
24. Kozlenkov A, Le Du MH, Cuniassé P, Ny T, Hoylaerts MF, Millan JL. Residues determining the binding specificity of uncompetitive inhibitors to tissue-nonspecific alkaline phosphatase. *J Bone Miner Res* 2004;19:1862-72.
25. Hoylaerts MF, Manes T, Millán JL. Mammalian alkaline phosphatases are allosteric enzymes. *J Biol Chem* 1997;272:22781-7.
26. Hui MZ, Tenenbaum HC, McCulloch CA. Collagen phagocytosis and apoptosis are induced by high level alkaline phosphatase expression in rat fibroblasts. *J Cell Physiol* 1997;172:323-33.
27. Mornet E. Hypophosphatasia: the mutations in the tissue-nonspecific alkaline phosphatase gene. *Hum Mutat* 2000;15:309-15.
28. Bodansky O. Mechanism of inhibition of phosphatase activity by glycine. *J Biol Chem* 1946;165:605-13.
29. Bodansky O. The inhibitory effects of DL-alanine, L-glutamic acid, L-lysine, and L-histidine on the activity of intestinal, bone and kidney phosphatases. *J Biol Chem* 1948;174:465-76.
30. Fishman W, Sie HG. L-homoarginine; an inhibitor of serum "bone and liver" alkaline phosphatase. *Clin Chim Acta* 1970;29:339-41.
31. Lin CW, Fishman WH. L-Homoarginine. An organ-specific, uncompetitive inhibitor of human liver and bone alkaline phosphohydrolases. *J Biol Chem* 1972;247:3082-7.
32. Fishman WH, Sie HG. Organ-specific inhibition of human alkaline phosphatase isoenzymes of liver, bone, intestine and placenta; L-phenylalanine, L-tryptophan and L-homoarginine. *Enzymologia* 1971;41:141-67.
33. Fishman WH, Green S, Inglis NR. L-Phenylalanine: An organ-specific, stereo-specific inhibitor of human intestinal alkaline phosphatase. *Nature* 1963;465:685-6.
34. Lin CW, Fishman WH. L-tryptophan. A non-allosteric organ-specific uncompetitive inhibitor of human placental alkaline phosphatase. *Biochem J* 1981;124:509-16.
35. Pritzker KPH. Calcium pyrophosphate crystal arthropathy. A biomineralization disorder. *Hum Pathol* 1986;17:543-5.
36. Cox RP, Macleod CM. Repression of alkaline phosphatase in human cell cultures by cystine and cysteine. *Proc Nat Acad Sci USA* 1963;49:504-10.
37. Agus SG, Cox RP, Griffin MJ. Inhibition of alkaline phosphatase by cysteine and its analogues. *Biochim Biophys Acta* 1966;118:363-70.
38. Zhu CM, Chen QC, Lin HN, et al. Kinetics of inhibition of green crab (*Scylla serrata*) alkaline phosphatase by L-cysteine. *J Protein Chem* 1999;18:603-7.
39. Vovk AI, Muzychka OV, Kharchenko OV. Kinetics and mechanism of interaction of L-cysteine with calf intestine alkaline phosphatase [Russian]. *Ukr Biokhim Zh* 2003;75:35-9.
40. Cordoba F, Nimni ME. Chondroitin sulfate and other sulfate containing chondroprotective agents may exhibit their effects by overcoming a deficiency of sulfur amino acids. *Osteoarthritis Cartilage* 2003;11:228-30.
41. Giles NM, Watts AB, Giles GI, Fry FH, Littlechild JA, Jacob C. Metal and redox modulation of cysteine protein function. *Chem Biol* 2003;10:677-93.
42. Fukagawa NK, Galbraith RA. Advancing age and other factors influencing the balance between amino acid requirements and toxicity. *J Nutr* 2004;134:1569S-74S.
43. Jacobs DS, DeMott WR, Oxley DK. *Laboratory test handbook*. 5th ed. Hudson, OH: Lexi-Comp Inc.; 2001.
44. Cheng P-T, Pritzker KPH, Adams ME, Nyburg SC, Omar SA. Calcium pyrophosphate crystal formation in aqueous solutions. *J Rheumatol* 1980;7:609-16.
45. Hase M. KaleidaGraph 3.0.5. for MacIntosh and Windows. Computer software reviews. *J Am Chem Soc* 1997;119:4323.
46. Kirsch PD, Ekerdt JG. KaleidaGraph: Graphing and data analysis. Version 3.5 for Windows. Computer software reviews. *J Am Chem Soc* 2000;122:11755.
47. Tommasini R, Endrenyi L, Taylor PA, Mahuran DJ, Lowden JA. A statistical comparison of parameter estimation for the Michaelis-Menten kinetics of human placental hexosaminidase. *Can J Biochem Cell Biol* 1985;63:225-30.
48. Hofstee BHJ. On the evaluation of the constants  $V_m$  and  $K_m$  in enzyme reactions. *Science* 1952;116:329-31.
49. Cortes A, Cascante M, Cardenas ML, Cornish-Bowden A. Relationships between inhibition constants, inhibitor concentrations for 50% inhibition and types of inhibition: new ways of analysing data. *Biochem J* 2001;357:263-8.
50. Cornish-Bowden A. A simple graphical method for determining the inhibition constants of mixed, uncompetitive and non-competitive inhibitors. *Biochem J* 1974;137:143-4.
51. Dixon M. The determination of enzyme inhibitor constants. *Biochem J* 1953;55:170-1.
52. Moss DW, Eaton RH, Smith JK, Whitby LG. Association of inorganic-pyrophosphatase activity with human alkaline-phosphatase preparations. *Biochem J* 1967;102:53-7.
53. Cox RP, Gilbert P Jr, Griffin MJ. Alkaline inorganic pyrophosphatase activity of mammalian-cell alkaline phosphatase. *Biochem J* 1967;105:155-61.
54. Xu Y, Cruz TF, Cheng P-T, Pritzker KPH. Effects of pyrophosphatase on dissolution of calcium pyrophosphate dihydrate crystals. *J Rheumatol* 1991;18:66-71.
55. Shinozaki T, Xu Y, Cruz TF, Pritzker KPH. Calcium pyrophosphate dihydrate (CPPD) crystal dissolution by alkaline phosphatase: interaction of alkaline phosphatase on CPPD crystals. *J Rheumatol* 1995;22:117-23.
56. Lawand NB, McNearney T, Westlund KN. Amino acid release into the knee joint: key role in nociception and inflammation. *Pain* 2000;86:69-74.
57. Giustarini D, Lorenzini S, Rossi R, Chindamo D, Di Simplicio P, Marcolongo R. Altered thiol pattern in plasma of subjects affected by rheumatoid arthritis. *Clin Exp Rheumatol* 2005;23:205-12.
58. Kozlenkov A, Manes T, Hoylaerts MF, Millán JL. Function assignment to conserved residues in mammalian alkaline

- phosphatases. *J Biol Chem* 2002;277:22992-9.
59. Samiec PS, Drews-Botsch C, Flagg EW, et al. Glutathione in human plasma: decline in association with aging, age-related macular degeneration, and diabetes. *Free Radical Biol Med* 1998;24:699-704.
  60. Giustarini D, Dalle-Donne I, Lorenzini S, Milzani A, Rossi R. Age-related influence on thiol, disulfide, and protein-mixed disulfide levels in human plasma. *J Gerontol A: Biol Sci Med Sci* 2006;61:1030-8.
  61. Hunter GK, Grynblas MD, Cheng P-T, Pritzker KPH. Effect of glycosaminoglycans on calcium pyrophosphate crystal formation in collagen gels. *Calcif Tissue Int* 1987;41:164-70.
  62. Bjelle AO. The glycosaminoglycans of articular cartilage in calcium pyrophosphate dihydrate (CPPD) crystal deposition disease (chondrocalcinosis articularis or pyrophosphate arthropathy). *Calcif Tissue Int* 1973;12:37-46.
  63. Galperin MY, Bairoch A, Koonin EV. A superfamily of metalloenzymes unifies phosphopentomutase and cofactor-independent phosphoglycerate mutase with alkaline phosphatases and sulfatases. *Protein Sci* 1998;7:1829-35.
  64. Gijsbers R, Ceulemans H, Stalmans W, Bollen M. Structural and catalytic similarities between nucleotide pyrophosphatases/phosphodiesterases and alkaline phosphatases. *J Biol Chem* 2001;276:1361-8.
  65. O'Brien PJ, Herschlag D. Sulfatase activity of *E. coli* alkaline phosphatase demonstrates a functional link to arylsulfatases, an evolutionarily related enzyme family. *J Am Chem Soc* 1998;120:12369-70.